Physica A 443 (2016) 568–582

Contents lists available at ScienceDirect

Physica A

journal homepage: www.elsevier.com/locate/physa

Partition signed social networks via clustering dynamics

Jianshe Wu *, Long Zhang, Yong Li, Yang Jiao

Key Laboratory of Intelligent Perception and Image Understanding of Ministry of Education of China, Xidian University, Xi'an 710071, China

HIGHLIGHTS

- A dynamic model describing the dynamics of signed social networks is provided.
- The dynamic model can be applied for partitioning signed social networks.
- A detailed algorithm is provided.
- The correctness and efficiency are verified on real-world and synthetic networks.

ARTICLE INFO

Article history:
Received 28 January 2015
Received in revised form 12 June 2015
Available online 8 October 2015

Keywords:
Graph partitioning
Signed social networks
Clustering dynamics
Community detection
Complex dynamical networks

ABSTRACT

Inspired by the dynamics phenomenon occurred in social networks, the WJJLGS model is modified to imitate the clustering dynamics of signed social networks. Analyses show that the clustering dynamics of the model can be applied to partition signed social networks. Traditionally, blockmodel is applied to partition signed networks. In this paper, a detailed dynamics-based algorithm for signed social networks (DBAS) is presented. Simulations on several typical real-world and illustrative networks that have been analyzed by the blockmodel verify the correctness of the proposed algorithm. The efficiency of the algorithm is verified on large scale synthetic networks.

1. Introduction

Social relations/links between actors may be positive or negative, for example, friendship/hostility, attract/exclude, like/dislike, and respect/disrespect between individuals [1,2]. The networks that include both positive and negative links are called signed social networks in the field of social science, and the networks with only positive links are called positive social networks [3,4]. Partitioning the signed social networks is quite different from partitioning the positive social networks, where the network is partitioned into several communities with dense links in each community and sparse links between communities [5–7]. By maximizing one of several cautiously defined criterion functions [8–10], the positive social networks can be properly partitioned via dedicatedly designed algorithms (known as community detection) [11–14]. On the other hand, it is well known that the dynamics of a network is correlated with its structure [15–17]. The community structure of a positive social network may be observed from the network dynamics [18–26] or cluster synchronization [27–30]. In cluster synchronization, the nodes in the same cluster are synchronized but desynchronized with respect to different clusters. Strict cluster synchronization usually requires a control scheme [27–30], thus it is difficult to be applied to community detection directly. In Ref. [24], the WJJLGS model is proposed to imitate the clustering dynamics of positive networks and used for community detection.

* Corresponding author. Tel.: +86 29 88202279.
E-mail address: jshwu@mail.xidian.edu.cn (J. Wu).

http://dx.doi.org/10.1016/j.physa.2015.09.066
0378-4371/

Clusters (or communities) in signed networks have dense positive intra-cluster links and only sparse positive inter-cluster links; in the same time they have dense negative inter-cluster links and only sparse negative intra-cluster links. Partitioning signed networks is also called correlation clustering problem [31]. Usually the signed networks are transformed to positive networks that can be treated with standard techniques by eliminating the negative links [32]. Of course, eliminating negative links means to give up useful information on the relationships between nodes. In order to design algorithms for signed networks, two modular functions were designed [33,34]. In Ref. [35], a Potts model was extended to incorporate negative links, and was applied to a network of international alliances and disputes. In Ref. [4], an agent-based heuristic algorithm named FEC was proposed for partitioning signed networks, and rigorous experiments were also done to verify the effectiveness of FEC. Recently, Chen et al. proposed a novel approach named signed probabilistic mixture (SPM) model, which provides soft memberships that can detect overlapping nodes of the communities [36]. In this paper, the proposed algorithm is compared with FEC and SPM by experiments.

The dynamics of the signed social networks is quite different from that of the positive social networks due to the negative links. A balanced signed network is defined that every closed loop is positive [37,38]. A closed loop in the network is said to be positive if it has even number of negative links. A balanced signed network can be partitioned into two clusters (communities) such that all the intra-cluster links are positive and all the inter-cluster links are negative (the first structure theorem presented by Cartwright and Harary [37,38]). But human population with signed links can be often split into more than two clusters. The concept of the balanced signed network is generalized by Davis [39]: a signed network is balanced (clusterable in his terminology) if it contains no closed loop with exactly one negative link. With the generalization, a balanced signed network can be partitioned into two or more communities such that all the intra-cluster links are positive and all the inter-cluster links are negative (the second structure theorem presented by Davis [39]). For clarity in this paper, a signed network is said to be clusterable if it is balanced in the generalized sense. In some references, the two concepts of balanced network are unified by the term "k-balanced network", $k \geqslant 2$.

But many real-world or artificial signed networks are not k-balanced (Chapter 10 in Ref. [40]). Blockmodeling approaches were developed to partition those un-balanced signed networks via minimizing a criterion (or measure) function across all possible partitions [40]. The criterion function is based on the line index of imbalance [41]:

$$\phi(C) = P_L + N_L,$$

where N_L is the total number of negative intra-cluster links and P_L is the total number of positive inter-cluster links. Minimizing $\phi(C)$ is equivalent to approaching the k-balanced partition as possible. A more general criterion function can be

$$\phi(C) = (1-\alpha)P_L + \alpha N_L, \quad 0 \leq \alpha \leq 1. \tag{1}$$

The positive inconsistencies are more important when $0 \leq \alpha < 0.5$. The negative inconsistencies are more important when $0.5 < \alpha \leq 1$. If $\alpha = 0.5$, the two inconsistencies are equally weighted. Doreian and Mrvar provided a local optimization algorithm to get a partition from minimizing $\phi(C)$ [3]. But the partition from minimizing the criterion function is problematic sometimes [42], which does not reflect the real structure of the network. Detailed examples can be found in Ref. [42]. Thus Doreian and Mrvar relaxed the structural balance blockmodel to accommodate more complex signed block structures. The relaxed structural balance blockmodel does not restrict positive blocks on the main diagonal and negative blocks off the main diagonal of the partitioned matrix. Recently, this approach was extended to large signed two-mode networks [43].

In this paper, the WJJLGS model is modified to imitate the clustering dynamics of signed social networks. Instead of the structural balance blockmodel, it is shown that the signed social networks can be partitioned via their clustering dynamics. In a social population, two individuals with positive interaction usually attract with each other in heart, and the distance between them in emotion gets smaller and smaller. On the other hand, two individuals with negative interaction usually exclude with each other in heart, and the distance between them in emotion gets longer and longer. A number of individuals with positive interactions form a community gradually. Individuals with negative interactions fall into different communities. In the modified WJJLGS model, individuals are represented by phase oscillators. The phases of two oscillators (individuals) with positive links approach to each other gradually, and the phases of two oscillators with negative links evolve far away from each other. Eventually, the phases of the oscillators are naturally split into several clusters. Thus a dynamics-based algorithm for signed networks (DBAS) partitioning is proposed.

2. The dynamical evolutionary model

The adjacency matrix $A = [a_{ij}]$ of a signed social network has three kinds of elements, $a_{ij} = 1$ ($a_{ij} = -1$) indicates a positive (negative) link, otherwise $a_{ij} = 0$ indicates no link. The original WJJLGS model is to imitate the clustering dynamics of positive networks [24], which is modified as follows to imitate the dynamics of signed social networks,

$$\frac{\mathrm{d}\theta_i}{\mathrm{d}t} = \frac{K_p}{N}\sum_{j=1}^{N}\frac{|a_{ij}|\,(1+a_{ij})}{2}\sin(\theta_j-\theta_i) + \frac{K_n}{N}\sum_{j=1}^{N}\frac{|a_{ij}|\,(1-a_{ij})}{2}\sin(\theta_j-\theta_i),$$
$$i = 1,\ldots,N,\ K_p > 0, K_n < 0, \tag{2}$$

where N is the number of nodes (individuals) in the positive social network, and θ_i is the phase of oscillator (node) i. The positive coupling strength K_p is to make the phases of two positively connected nodes ($a_{ij} = 1$) in the network evolve

together; the negative coupling strength K_n is to make the phases of two negatively connected nodes ($a_{ij} = -1$) in the network evolve far away. The maximum phase difference of two nodes is π: $\max\{|\theta_i - \theta_j|\} = \pi$, $\theta_i - \theta_j \in [-\pi, \pi]$. Suppose a two-node network is positively linked and $\theta_2(0) > \theta_1(0)$ at time $t = 0$, then from (2)

$$\frac{d\theta_1}{dt} = \frac{K_p}{2}\sin(\theta_2 - \theta_1) > 0,$$

$\theta_1(t)$ evolve close to $\theta_2(t)$. Similarly

$$\frac{d\theta_2}{dt} = \frac{K_p}{2}\sin(\theta_1 - \theta_2) < 0,$$

$\theta_2(t)$ evolve close to $\theta_1(t)$ until $\theta_1(t) = \theta_2(t)$. That is, the phases of the two nodes evolve together. For a connected graph consisting of three or more positively linked nodes, identical analysis shows that the phases also approach together.

On the other hand, the purpose of the negative coupling strength K_n is to make the phases of two negatively linked oscillators ($a_{ij} = -1$) in the network evolve far away. Suppose a two-node network is negatively linked and $\theta_2(0) > \theta_1(0)$ at time $t = 0$, then from (3)

$$\frac{d\theta_1}{dt} = \frac{K_n}{2}\sin(\theta_2 - \theta_1) < 0,$$

$\theta_1(t)$ evolve far away from $\theta_2(t)$. Similarly

$$\frac{d\theta_2}{dt} = \frac{K_n}{2}\sin(\theta_1 - \theta_2) > 0,$$

$\theta_2(t)$ evolve far away from $\theta_1(t)$. For three or more negatively linked nodes, their phases evolve far away in $[0, 2\pi]$.

If there is no link between node i and $j(a_{ij} = 0)$, then $|a_{ij}| = 0$, both K_p and K_n have no effect on the evolution of the phases. In the simulations of this paper, the initial phases θ_i are randomly distributed in $[0, 2\pi)$ and mod 2π is applied in the computation.

3. Dynamics of the model

3.1. Dynamics of the balanced networks

Theorem 1. *For a balanced signed network, after a period of evolution by (2), the phases of the nodes can be stabilized into two constant values (θ^1, θ^2) corresponding to two communities (clusters), any two positively linked nodes are in the same community and any two negatively linked nodes are in different communities. Furthermore, the two stable phases satisfy*

$$\theta^1 - \theta^2 = \pm\pi. \tag{3}$$

Proof. A balanced network can be partitioned into two communities, so that all the positively linked nodes (plus-set in term of Ref. [39]) are in the same community and any two negatively linked nodes are in different communities (see Theorem 1 in Ref. [42]). From (2), the phases of all the positively linked oscillators (nodes) can evolve together by the positive coupling strength K_p until they reach a consensus. Thus the phases of the two communities reach two values $(\theta^1(t), \theta^2(t))$ respectively. From (2), the phases of any two negatively linked nodes evolve far away by the negative coupling strength K_n. Thus the phases of the two communities (which are negatively linked) evolve far away gradually. Since the period of sine function is 2π, that is, the phases of all the nodes be distributed in $[0, 2\pi]$, the farthest distance between θ^1 and θ^2 is π. Thus Eq. (3) holds.

After the phases of the two communities (denoted as C_1 and C_2) reach consensus respectively, one has $\theta_i(t) - \theta_j(t) = 0$ if nodes i and j are in the same community, or $\theta_i(t) - \theta_j(t) = \pm\pi$ if nodes i and j are in different communities. For both cases, from (2) one has $d\theta_i(t)/dt = 0$ for $i = 1, \ldots, N$.

Example 1. Dynamics of a balanced network.

Consider a balanced signed network with 10 nodes as shown in Fig. 1. The partitioned adjacency matrix of the network is shown in Table 1. Obviously, the network can be partitioned into two communities C_1 and C_2. Because all the links among the nodes in C_1 are positive (see Table 1), from (2) the phases evolve together gradually. Identically, the phases of the nodes in C_2 also evolve together gradually. But the links between the nodes in different communities are negative (see Table 1), thus the phases of the two communities evolve far away. Fig. 2 is the simulation result of (2) when $K_p = 14$ and $K_n = -5$. As shown in Fig. 2, after about $t = 2$ s of dynamical evolution (t is not the run time of the program, but the t in (2)), the phases of the nodes are stable and divided into two communities: $C_1 = \{1, 2, 3, 4, 5\}$ and $C_2 = \{6, 7, 8, 9, 10\}$. The stable phases of the two communities are $\theta^1 = 1.7194$ and $\theta^2 = 4.8610$ respectively, $\theta^2 - \theta^1 = 3.1416$.

For a balanced network, Theorem 1 indicates that it can be easily partitioned into two communities by setting K_p any positive number and K_n any negative number, with only positive links in community and only negative links between the two communities.

Table 1
Partitioned matrix of the signed social network shown in Fig. 1.

	1	2	3	4	5	6	7	8	9	10
1	0	1	0	0	1	0	0	0	0	−1
2	0	0	0	1	0	−1	−1	0	0	0
3	1	1	0	1	1	0	0	0	−1	0
4	0	0	1	0	1	0	0	−1	−1	0
5	1	1	0	0	0	0	0	−1	0	−1
6	0	−1	0	−1	0	0	0	1	1	0
7	0	0	0	0	−1	1	0	1	0	1
8	−1	0	−1	0	−1	0	1	0	1	1
9	0	0	−1	0	0	0	1	1	0	0
10	−1	0	−1	0	−1	0	1	1	1	0

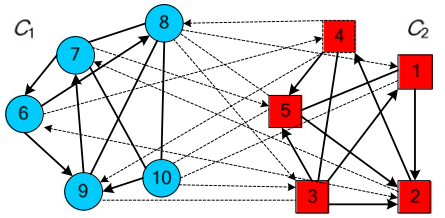

Fig. 1. A balanced signed network with 10 nodes.

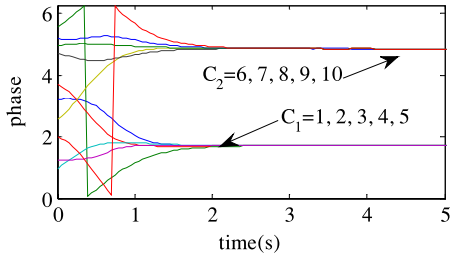

Fig. 2. Simulation results on the network shown in Fig. 1. The phases evolving with time when $K_p = 14$ and $K_n = -5$ are illustrated in Fig. 2; they are stabilized into two values: $\theta^1 = 1.7194$ and $\theta^2 = 4.8610$. $\theta^2 - \theta^1 = 3.1416$.

3.2. Dynamics of the clusterable networks

Theorem 2. *For a clusterable signed network, after a period of evolution by (2), the phases of the nodes can be stabilized into k values $(\theta^1, \theta^2, \ldots, \theta^k)$ corresponding to k communities (clusters), $k \geqslant 2$. Any two positively linked nodes are in the same community and any two negatively linked nodes are in different communities.*

Proof. A clusterable network can be partitioned into k communities, $k \geqslant 2$, so that all the positively linked nodes are in the same community and any two negatively linked nodes are in different communities (see Theorem 2 in Ref. [42]). From (2), the phases of all the positively linked oscillators can evolve together by the positive coupling strength K_p until they reach consensus. The phases of the k communities reach k values $(\theta^1(t), \theta^2(t), \ldots, \theta^k(t))$ respectively. From (2), the phases of any two negatively linked nodes evolve far away by the negative coupling strength K_n. Thus the phases of the k communities (which are negatively linked) evolve far away gradually until balance is reached.

Example 2. Dynamics of a clusterable network.

Consider a clusterable signed network with 20 nodes as shown in Fig. 3. The partitioned adjacency matrix of the network is shown in Table 2. The network can be partitioned into four communities: C_1, C_2, C_3, and C_4. All the intra-community links are positive and all the inter-community links are negative. Fig. 4 is the simulation result of (2) when $K_p = 20$ and $K_n = -1$. As shown in Fig. 4, the phases of the nodes in each community gradually evolve together. The phases of the entire network evolve into four different values corresponding to four communities: $C_1 = \{1, 2, 3, 4, 5\}$, $C_2 = \{6, 7, 8, 9, 10\}$, $C_3 = \{11, 12, 13, 14, 15, 16\}$, and $C_4 = \{17, 18, 19, 20\}$.

Identical as that of Theorem 1, for a clusterable network, Theorem 2 indicates that it can be easily partitioned into two or more communities by setting K_p any positive number and K_n any negative number, with only positive links in community and only negative links between the communities. Theorems 1 and 2 indicate that the proposed methodology completely coincides with the traditional structural balance theory.

Table 2
Partitioned matrix of the signed social network shown in Fig. 3.

	1	2	3	4	5	6	7	8	9	10	11	12	13	14	15	16	17	18	19	20
1	0	1	0	1	1	0	−1	−1	0	0	0	0	0	0	−1	0	0	0	0	0
2	1	0	1	0	1	0	−1	0	0	0	0	−1	0	0	0	0	0	0	0	0
3	1	1	0	1	1	−1	0	0	0	0	0	0	0	0	0	0	0	0	0	0
4	1	1	1	0	0	−1	−1	0	0	0	0	0	−1	0	−1	0	0	1	−1	0
5	1	1	1	0	0	0	−1	0	0	0	−1	−1	−1	0	−1	0	0	0	0	0
6	0	0	−1	−1	0	0	1	1	1	1	0	0	−1	0	0	0	0	0	0	0
7	0	−1	0	−1	−1	1	0	0	1	1	0	−1	0	−1	0	0	0	0	0	0
8	−1	0	0	−1	0	1	1	0	1	1	−1	0	0	0	0	0	0	0	0	0
9	0	0	0	0	0	1	1	0	0	0	0	−1	0	−1	0	0	0	−1	−1	0
10	0	0	0	0	0	1	1	1	0	0	0	0	0	0	0	0	0	0	0	0
11	0	0	0	0	−1	0	0	−1	0	−1	0	1	1	0	0	1	0	0	−1	0
12	0	−1	0	0	−1	0	−1	0	−1	0	1	0	1	1	1	1	0	0	0	0
13	0	0	0	−1	−1	0	−1	0	0	0	1	1	0	1	1	0	−1	0	0	0
14	0	0	−1	0	0	0	−1	0	−1	0	0	1	1	0	1	1	0	0	0	0
15	−1	0	0	−1	0	0	0	0	0	0	0	1	0	1	0	1	0	0	0	0
16	0	0	0	0	0	0	0	0	0	0	1	1	0	1	0	0	0	0	0	0
17	0	0	0	0	0	0	0	0	0	0	0	0	0	0	0	0	0	1	1	1
18	0	0	0	0	0	0	0	−1	−1	0	0	0	0	−1	0	0	1	0	0	1
19	0	−1	0	0	0	0	0	0	0	0	−1	0	0	0	0	0	1	1	0	1
20	0	0	0	0	0	0	0	0	0	0	0	0	0	0	0	0	1	0	1	0

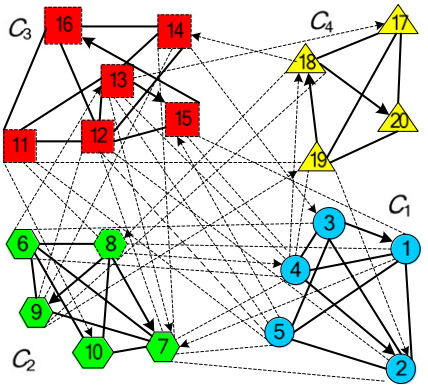

Fig. 3. A clusterable signed network with 10 nodes.

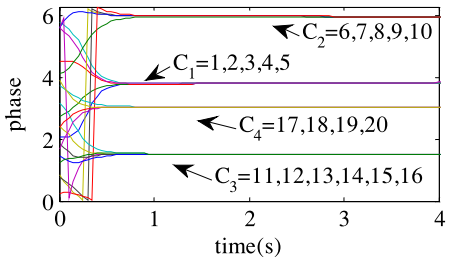

Fig. 4. The phases of the nodes shown in Fig. 3 evolving with time by (2) when $K_p = 20$ and $K_n = -1$; they are stabilized into four lines.

The dynamics of the proposed model on balanced and clusterable networks are really cluster synchronization [29,30], where the phases in the same cluster are synchronized and the phases in different clusters are not. Cluster synchronization in networks is usually achieved by using a control scheme [27–30].

3.3. Dynamics of general networks

For a general signed social network in the sense that it is neither balanced nor clusterable, it may have two types of inconsistent links: negative intra-community links and positive inter-community links when it is partitioned. The negative

Table 3
Partitioned matrix of the signed social network shown in Fig. 5.

	1	2	3	4	5	6	7	8	9	10	11	12	13	14
1	0	1	1	0	0	1	0	0	−1	0	0	0	0	0
2	0	0	1	1	0	1	−1	0	0	−1	0	0	0	0
3	1	1	0	1	1	0	−1	−1	−1	0	0	0	[1]	0
4	0	0	1	0	0	1	−1	−1	0	−1	0	0	0	[1]
5	1	1	0	0	0	1	0	0	−1	−1	[1]	0	0	0
6	0	1	0	1	0	0	0	−1	0	−1	0	[1]	0	0
7	−1	−1	−1	0	0	0	0	1	1	1	0	[1]	[1]	0
8	0	0	−1	−1	0	−1	1	0	0	1	0	0	0	0
9	−1	−1	0	−1	−1	0	1	1	0	1	0	[1]	0	0
10	0	0	0	−1	−1	−1	1	0	1	0	[1]	0	0	0
11	0	0	0	[1]	0	0	0	0	0	[1]	0	1	1	0
12	0	0	0	0	0	0	0	[1]	0	0	1	0	1	1
13	0	0	0	0	[1]	[1]	[1]	0	0	0	1	1	0	1
14	0	0	0	0	[1]	0	0	0	[1]	0	1	1	1	0

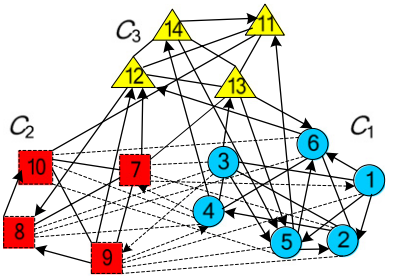

Fig. 5. A general signed network with 14 nodes.

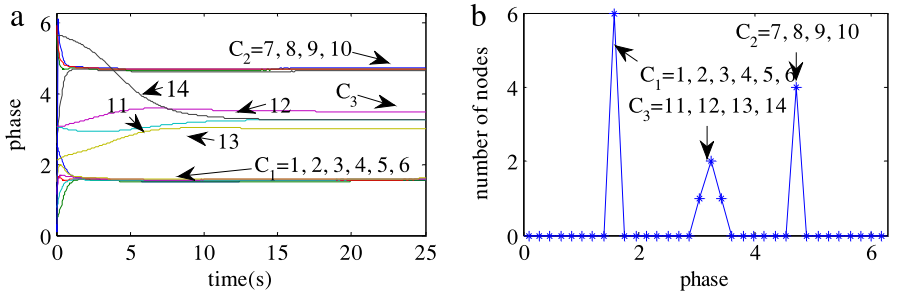

Fig. 6. Simulation results of the network shown in Fig. 5. (a) The phases of the nodes evolving by (2). (b) Distribution of the stable phases in $[0, 2\pi]$.

intra-community links make it hard for the phases of the community to reach consensus. The positive inter-community links make it hard for the phases of the two communities to reach consensus respectively.

Example 3. Dynamics of a general network.

As shown in Fig. 5, consider a network consisting of 14 nodes that is partitioned into three communities: $C_1 = \{1, 2, 3, 4, 5, 6\}$, $C_2 = \{7, 8, 9, 10\}$, and $C_3 = \{11, 12, 13, 14\}$. The partitioned adjacency matrix of the network is shown in Table 3, wherein the 16 inconsistent links are boxed. It is seen that community C_3 is positively linked with C_1 and C_2. The nodes of C_3 are viewed as potential mediators. The phases of the nodes evolving by (2) are shown in Fig. 6(a) when $K_p = 2$ and $K_n = -25$, which shows that the phases of each community are no longer equal but close to each other, and the phases in different communities are far away relatively. By dividing $[0, 2\pi]$ into 20 equal subintervals and calculating the number of nodes whose stable phases fall into the subintervals, the distribution curve is shown in Fig. 6(b). A peak in Fig. 6(b) corresponds to a community, and the signed network can be easily partitioned into three communities from Fig. 6(b).

It is seen from Fig. 6 that the structure of a general signed social network is also revealed by the dynamics. The phases of the nodes are split into several clusters corresponding to a partition of the network, though the phases in each cluster are not strictly equal.

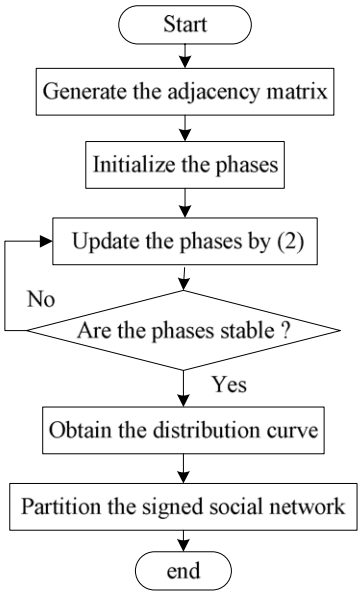

Fig. 7. The flow chart of the algorithm.

In summary: (i) for a balanced network, the phases of the nodes can be split into two clusters. The phases in each cluster are strictly equal and (3) holds. (ii) For a clusterable network, the phases of the nodes can be split into two or more clusters. The phases in each cluster are strictly equal. (iii) For a general network that has inconsistent links, the phases of the nodes can be split into two or more clusters. The phases in each cluster may not be strictly equal but are close to each other, whereas the phases in different clusters are far away. Thus, a signed network can be partitioned via its dynamics. Detailed algorithm is presented in the next section.

4. The procedure of DBAS

Fig. 7 is the flow chart of the algorithm for partitioning via dynamics.

Step 1: Generate the adjacency matrix of the signed network.

If node i is positively linked with node j, then $a_{ij} = 1$ in the adjacency matrix $[a_{ij}]$; if node i is negatively linked with node j, then $a_{ij} = -1$; otherwise $a_{ij} = 0$. For a weighted (valued) signed network, a_{ij} is not limited to 1 and -1.

Step 2: Initialize the phase of the nodes.

Randomly generate an initial phase in $[0, 2\pi]$ for each of the nodes.

Step 3: Update the phases of the nodes by Eq. (2).

Set two values for the two parameters K_p and K_n, and update the phases of nodes by (2) until the phases are stable. Identical as the parameter α in (1), K_p and K_n control the weights of the two inconsistencies. Mod 2π is applied in the calculation to ensure that each phase keeps in $[0, 2\pi]$. The following criterion is used to determine whether the phases are stable: $\theta_i(t) - \theta_i(t-\tau) < \varepsilon$, where ε is a small positive value and τ is a time delay. For example, $\varepsilon = 0.001$ and $\tau = 3$ are usually used in the simulations of this paper, representing that the phase difference of node i is less than 0.001 in the three seconds.

Step 4: Obtain the distribution curve of the stable phases (see Fig. 6(b) as an example).

Divide $[0, 2\pi]$ into l sub-intervals with equal length $2\pi/l$ and calculate the number of nodes whose stable phases fall into each sub-interval. The value of l is related with the number of communities in the network, more communities in the network require a larger value of l usually. In the experiments of this paper, $l = 40$.

Step 5: Partition the signed social network according to the distribution of the stable phases.

Merge the nodes in adjacent sub-intervals into a group if the number of nodes in each sub-interval is not zero. Two groups are separated by one (or more) sub-interval whose number of nodes is zero (see Fig. 6(b) as an example). To be specific, all the points of zero vertical ordinate in the distribution curve of the stable phases separate the nodes into several groups (in Fig. 6(b), it is separated into three groups). Calculate the number of nodes (N_group) in each group. Usually, some groups have only one or two nodes, which are not regarded as communities in general. The parameter N_{th} is given as a threshold to judge whether a group have enough nodes to be a community. If $N\_\text{group} \geqslant N_{th}$, then the group is a community; Otherwise, these nodes are overlapping (mediating) nodes and assigned into other communities according to the ratio of the number of positive links to that of negative links.

Table 4
Partitioned matrix of the Gahuku-Gama subtribes network.

	1	2	15	16	5	9	10	13	14	3	4	6	7	8	11	12
1 GAVEV	0	1	1	1	−1	0	0	0	0	−1	−1	−1	0	0	0	−1
2 KOTUN	1	0	1	1	−1	−1	−1	0	0	−1	0	−1	0	0	0	0
15 NAGAD	1	1	0	1	−1	−1	−1	−1	0	0	0	0	0	0	−1	−1
16 GAMA	1	1	1	0	−1	0	0	−1	−1	0	0	−1	0	0	−1	−1
5 NAGAM	−1	−1	−1	−1	0	1	0	0	1	0	0	0	1	0	0	0
9 NOTOH	0	−1	−1	0	1	0	1	1	0	0	0	−1	0	0	−1	0
10 KOHIK	0	−1	−1	0	0	1	0	1	0	0	0	0	0	0	−1	0
13 UHETO	0	0	−1	−1	0	1	1	0	1	0	0	−1	1	0	−1	0
14 SEUVE	0	0	0	−1	1	0	0	1	0	0	0	0	0	−1	0	−1
3 OVE	−1	−1	0	0	0	0	0	0	0	0	1	1	1	1	0	0
4 ALIKA	−1	0	0	0	0	0	0	0	0	1	0	0	0	1	0	0
6 GAHUK	−1	−1	0	−1	0	−1	0	−1	0	1	0	0	1	1	1	1
7 MASIL	0	0	0	0	1	0	0	1	0	1	0	1	0	1	1	1
8 UKUDZ	0	0	0	0	0	0	0	0	−1	1	1	1	1	0	1	1
11 GEHAM	0	0	−1	−1	0	−1	−1	−1	0	0	0	1	1	1	0	1
12 ASARO	−1	0	−1	−1	0	0	0	0	−1	0	0	1	1	1	1	0

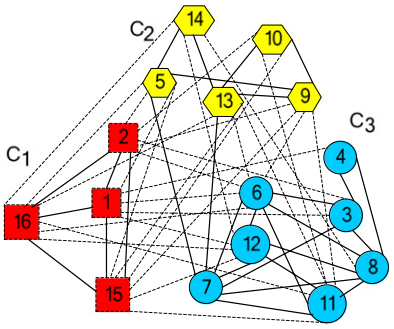

Fig. 8. The Gahuku-Gama subtribes network. The names of the subtribes can be seen in Table 4.

The most computational time of the proposed DBAS is costed in the evolution of (2), which is increased in a quadratic relation with the network scale N. The computational time of one node evolution by (2) can be estimated as βd, where d is the degree of the node and β is a coefficient. Then the computational time of the N nodes is about $\beta \bar{d} N$, where $\bar{d}$ is the average degree of the network. In the worst case, $\bar{d} = N$, thus the time complexity is $O(N^2)$.

5. Simulations

5.1. Simulations on real-world and illustrative networks

Simulation 1. The Gahuku-Gama subtribes network. The real-world network comes from the research about the cultures of New Guinea Highland [44], which describes the political alliances and oppositions among 16 Gahuku-Gama subtribes. As shown in Fig. 8, the political relationships among the subtribes may be positive or negative.

The adjacency matrix of the network is shown in Table 4. Fig. 9 is the simulation results by (2) when $K_p = 20$ and $K_n = -10$. The network is partitioned into three communities with the dynamics algorithm ($N_{th} = 3$): C_1 = {NAGAD, GAMA, GAVEV, KOTUN}, C_2 = {NAGAM, UHETO, KOHIK, NOTOH, SEUVE}, and C_3 = {ASARO, GEHAM, OVE, UKUDZ, GAHUK, MASIL, ALIKA}. The partition result is identical to the analysis result given by Doreian and Mrvar [3].

Simulation 2. The Slovene parliamentary parties network.

As the name indicates, the data of the network come from the elected members of the Slovene National Parliament [45]. The network presents the relations of 10 parties of the Slovene Parliament in 1994, which was established by a group of experts on Parliament activities. Fig. 10 shows the graph of the network. The adjacency matrix is shown in Table 5.

The phases of the nodes evolving with time are shown in Fig. 11 when $K_p = 16$ and $K_n = -10$. The stable phases of the nodes are divided into two clusters. Applying the algorithm with $N_{th} = 3$, the network is partitioned into two communities: C_1 = {SLS, SPS − SNS, SKD, ZS, SDSS} and C_2 = {LDS, DS, ZS − ESS, ZLSD, SNS}. The partition result is identical to the analysis result given by Kropivnik and Mrvar [46].

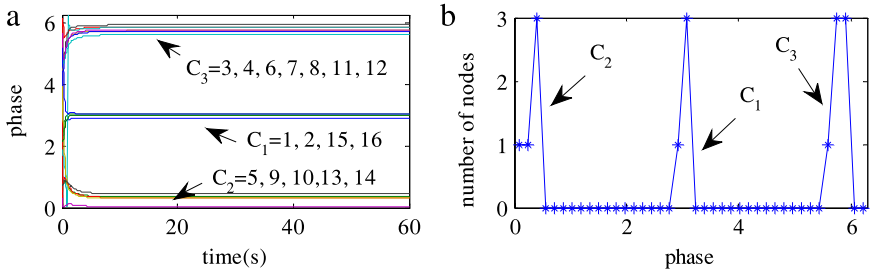

Fig. 9. Simulation results of the Gahuku-Gama subtribes network. (a) The phases of the nodes evolving by (2). (b) Distribution of the stable phases in $[0, 2\pi]$.

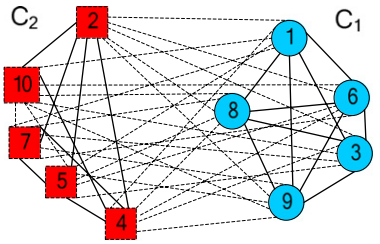

Fig. 10. The Slovene parliamentary parties network. The names of the parties can be seen in Table 5.

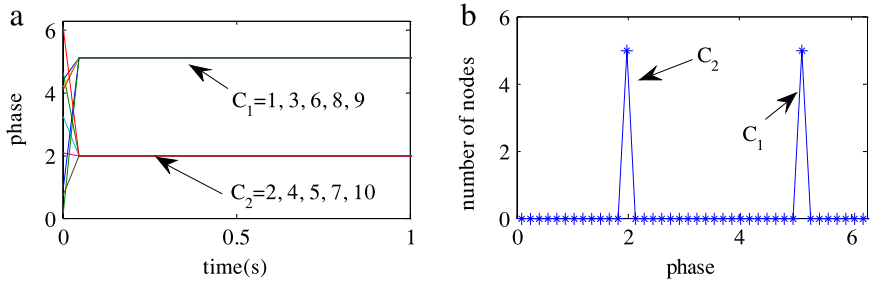

Fig. 11. Simulation results of the Slovene parliamentary parties network. (a) The phases of the nodes evolving by (3). (b) Distribution of the stable phases in $[0, 2\pi]$.

Table 5
Partitioned matrix of the Slovene parliamentary parties network.

	1	3	6	8	9	2	4	5	7	10
1 SKD	0	114	94	176	117	−215	−89	−77	−170	−210
3 SDSS	114	0	138	117	180	−217	−203	−80	−109	−174
6 ZS	94	138	0	140	116	−150	−142	−188	−97	−106
8 SLS	176	177	140	0	235	−253	−241	−120	−184	−132
9 SPS-SNS	117	180	116	235	0	−230	−254	−160	−191	−164
2 ZLSD	−215	−217	−150	−253	−230	0	134	77	57	49
4 LDS	−89	−203	−142	−241	−254	134	0	157	173	23
5 ZS-ESS	−77	−80	−188	−120	−160	77	157	0	170	-9
7 DS	−170	−109	−97	−184	−191	57	173	170	0	-6
10 SNS	−210	−174	−106	−132	−164	49	23	-9	-6	0

Simulation 3. Two illustrative signed networks.

The two illustrative signed networks are depicted in Fig. 12(a) and (b) respectively, which come from Ref. [4]. The network in Fig. 12(a) is clusterable, which can be partitioned into three communities without inconsistent links: $C_1 = \{6, 7, 22, 23, 24, 25, 13, 14, 15, 16, 4, 5\}$, $C_2 = \{20, 21, 10, 11, 12, 1, 2, 3, 19, 28\}$, and $C_3 = \{8, 9, 26, 27, 17, 18\}$. The network is also balanced because it can be partitioned into two communities without inconsistent links: $C_1 = \{6, 7, 22, 23, 24, 25, 13, 14, 15, 16, 4, 5\}$ and $C_2 + C_3 = \{8, 9, 26, 27, 17, 18, 20, 21, 10, 11, 12, 1, 2, 3, 19, 28\}$ [4]. Applying the dynamics algorithm, the network is also partitioned into two or three communities depending on the value of K_p and K_n. In a wide range of K_p, if $K_n < -0.15$, the network is partitioned into two communities. Fig. 13(a) is a simulation

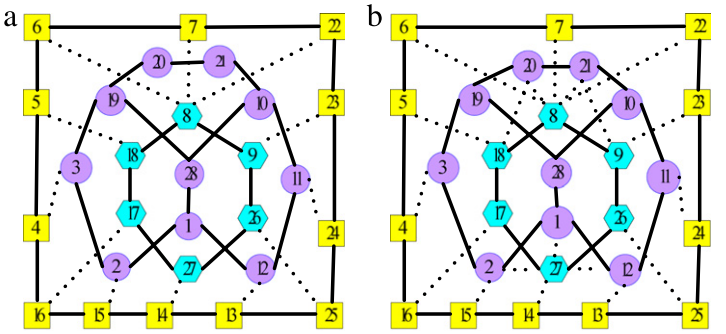

Fig. 12. Two illustrative networks. (a) The network is both balanced and clusterable. (b) The network is clusterable; however, it is not balanced.

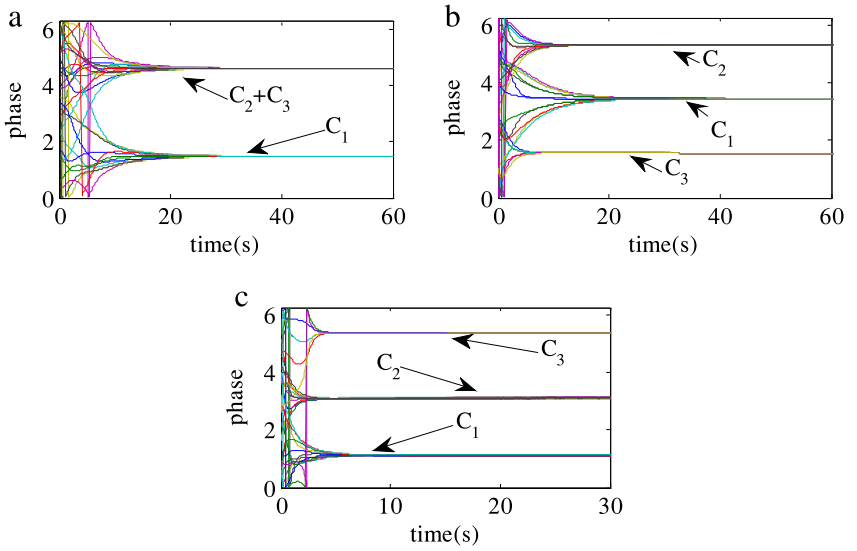

Fig. 13. Simulation results of the two illustrative networks. (a) The phases of the network shown in Fig. 12(a) evolving with time when $K_p = 20$ and $K_n = -0.2$. (b) The phases of the network shown in Fig. 12(a) evolving with time when $K_p = 20$ and $K_n = -0.01$. (c) The phases of the network shown in Fig. 12(b) evolving with time when $K_p = 60$ and $K_n = -1.8$.

result when $K_p = 20$ and $K_n = -0.2$. If $K_n > -0.05$, then it is partitioned into three communities. Fig. 13(b) is a simulation result when $K_p = 20$ and $K_n = -0.01$. Though there is no link between C_2 and C_3, both of them are negatively linked with C_1. Larger value of K_n makes them evolve far away from C_1 and eventually merge together. Smaller value of K_n makes them evolve far away from C_1 but is not sufficient to merge together. For this network, resulting in two or three communities also has relation with the initial phases of the nodes. For example, let $K_p = 20$ and $K_n = -0.13$. We run the algorithm 1000 times with randomly generated initial phases; in 583 times the network is partitioned into two communities and in 417 times it is partitioned into three communities.

The network shown in Fig. 12(b) is clusterable but not balanced, which is modified from Fig. 12(a) by adding 7 negative links between C_2 and C_3. Applying the dynamics algorithm, the network is always partitioned into three communities. Fig. 13(b) is a simulation result when $K_p = 60$ and $K_n = -1.8$.

Simulation 4. The US Supreme Court network.

The US Supreme Court network is shown in Fig. 14, which is taken from the voting behavior of the nine justices for making decisions on the US Supreme Court for the 2006–2007 term [42]. The adjacency matrix of the network is shown in Table 6. The elements in the main diagonal of the matrix are the number of votes made by the justices in these decisions. The off diagonal elements are net counts of the number of times justices vote for each other (if positive), or the number of times justices vote against each other (if negative).

In the previous literature, the network was partitioned into three communities or two communities [42]. The three-community partition divides the court into a liberal wing (Stevens, Ginsburg, Souter, Breyer) and a conservative wing (Alito, Roberts, Scalia, Thomas) with Justice Kennedy (represented by node 5) aligned between them. The two-community partition divides Justice Kennedy into the conservative wing of the court, which is consistent with the fact. Fig. 15 is the simulation results of the dynamics algorithm when $K_p = 17$ and $K_n = -1.2$. The network is partitioned into two communities when

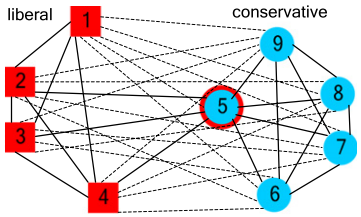

Fig. 14. The US Supreme Court network, each node represents a justice in the Supreme Court. The names of the justices can be seen in Table 6.

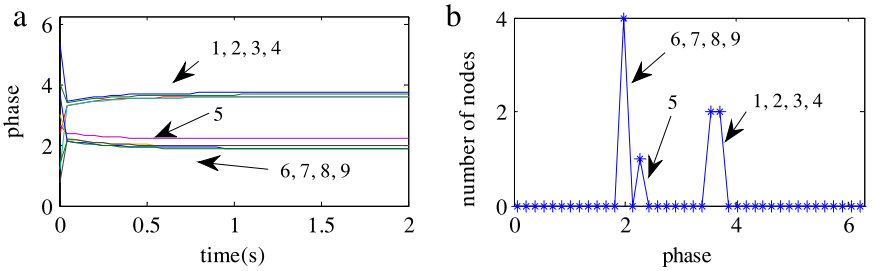

Fig. 15. Simulation results of the US Supreme Court network when $K_p = 17$ and $K_n = -1.2$. (a) The phases of the nodes evolving by (2). (b) Distribution of the stable phases in $[0, 2\pi]$.

Table 6
Partitioned matrix of the US Supreme Court network.

	1	2	3	4	5	6	7	8	9
1 Stevens	46	30	16	21	−7	−18	−17	−26	−31
2 Ginsburg	30	46	28	29	1	−10	−11	−18	−21
3 Souter	16	28	46	29	7	−4	−1	−16	−19
4 Breyer	21	29	29	45	10	−5	−6	−21	−24
5 Kennedy	−7	1	7	10	45	29	24	9	8
6 Alito	−18	−10	−4	−5	29	46	33	22	19
7 Roberts	−17	−11	−1	−6	24	33	45	29	24
8 Scalia	−26	−18	−16	−21	9	22	29	46	37
9 Thomas	−31	−21	−19	−24	8	19	24	37	45

$4 \geqslant N_{th} \geqslant 2$. If $N_{th} = 1$ (one node can be a community), the network is partitioned into three communities. From Table 6, Justice Kennedy has positive links with all the justices of the conservative wing, has three positive links and a negative link with the liberal wing. In fact, Justice Kennedy bridges the two communities as a mediator, which can be observed in Fig. 15.

5.2. Simulations on synthetic networks

Generate synthetic networks. Identical as the method to generate synthetic signed networks introduced by Wu et al. [46], synthetic networks are generated to test the dynamics algorithm. First, generate k communities of the network. Each of the communities is generated by the well-known Barabási and Albert (BA) scale-free model [47]. Scale-free networks are widely observed in social and biological networks. The BA model generates random scale-free networks using a preferential attachment mechanism. Commencing with an initial positively linked network of m_0 nodes, a new node is added to the network at each time until the community size is satisfied. Each new node is positively linked to m existing nodes ($m \leqslant m_0$) with a probability that is proportional to the number of links that the existing nodes already possess. Second, the k communities are connected by negative links. Define p as the ratio of the number of inter-community negative links to that of the intra-community positive links. If $p = 0$ there is no inter-community negative links. If $p = 1$, the inter-community negative links and intra-community positive links possess the same size. Eventually, a k-balanced network is generated. Third, randomly flip the signs of the existing links with probability q. If $q \neq 0$, an un-balanced signed network is generated.

Simulation 5. Six synthetic networks.

In this simulation, $m_0 = 5$ and $m = 4$, four networks are generated with $N = 1000$ and two with $N = 3000$. The values of the rest parameters are given in the caption of Fig. 16. Fig. 16 shows the distribution of the stable phases in $[0, 2\pi]$. The term "$C_1 = 110$" in the caption presents that community C_1 has 110 nodes. The six networks are correctly partitioned with the dynamics algorithm.

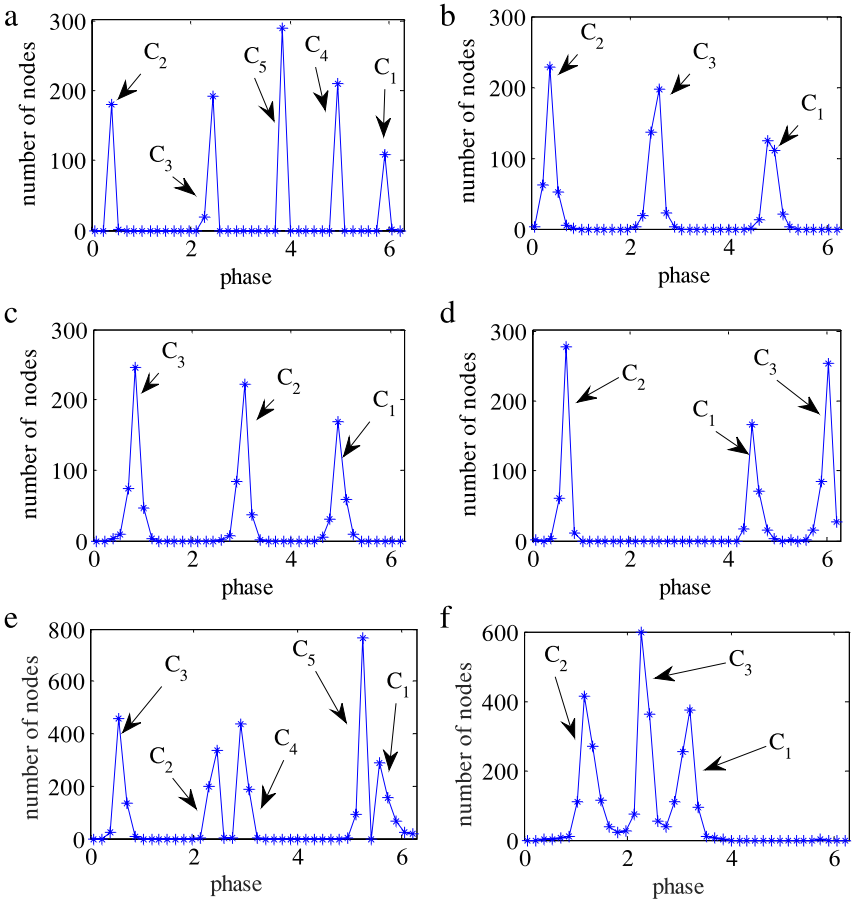

Fig. 16. Distribution of the stable phases in $[0, 2\pi]$ for the synthetic 1000-node and 3000-node networks. (a) $N = 1000$, $C_1 = 110$, $C_2 = 180$, $C_3 = 210$, $C_4 = 210$, $C_5 = 290$, $p = 0.6$, $q = 0$, $K_p = 15$, and $K_n = -0.9$. (b) $N = 1000$, $C_1 = 270$, $C_2 = 350$, $C_3 = 380$, $p = 0.6$, $q = 0.1$, $K_p = 10$, and $K_n = -1$. (c) $N = 1000$, $C_1 = 270$, $C_2 = 350$, $C_3 = 380$, $p = 0.6$, $q = 0.15$, $K_p = 11$, and $K_n = -1.1$. (d) $N = 1000$, $C_1 = 300$, $C_2 = 330$, $C_3 = 370$, $p = 0.2$, $q = 0.2$, $K_p = 10$, and $K_n = -1.1$. (e) $N = 3000$, $C_1 = 330$, $C_2 = 540$, $C_3 = 630$, $C_4 = 630$, $C_5 = 870$, $p = 0.6$, $q = 0$, $K_p = 15$, $K_n = -1.5$. (f) $N = 3000$, $C_1 = 900$, $C_2 = 990$, $C_3 = 1110$, $p = 0.2$, $q = 0.2$, $K_p = 15$, $K_n = -1.5$.

Table 7
Run time of the four 3000-nodes networks in Simulation 5.

(K_p, K_n)	(3, −0.3)	(15, −1.5)	(75, −7.5)	(150, −15)
Run time (s)	246	1204	6454	13 297

We test the run time of the proposed DBAS on four 3000-node networks with different values of K_p and K_n (include the two networks whose simulation results are shown in Fig. 16(e) and (f)). The partition results are almost the same, but the run times are different as shown in Table 7. If we further change the values of (K_p, K_n) to $(1, -0.1)$ the run time is very long and the memory is overflow in a 6G memory computer. DBAS works well in a very wide range of K_p and K_n, smaller values of K_p and $|K_n|$ result in faster speed usually, but too small of K_p and $|K_n|$ will make the differential equation difficult to reach convergence.

Simulation 6. Comparative experiments.

In this simulation, we comparatively test the performance of the proposed algorithm on networks of $N = 65$ and $N = 300$ with different values of q (see Fig. 17). The other parameters of the networks are $m_0 = 4$ and $m = 3$, and $p = 0.6$. The performance of the algorithms are evaluated by the error rate defined in Ref. [4] and the criterion function $\phi(C)$ defined by (1). The smaller the value of error rate and $\phi(C)$, the better the quality of the partition. Each point of Fig. 17 is an average tested on 10 networks.

Besides FEC and SPM, the dynamics-based algorithm for positive networks (DBAP) proposed in Ref. [24] is also tested in the experiments by ignoring the negative links; the values of K_p and K_n are always equal to that of DBAS.

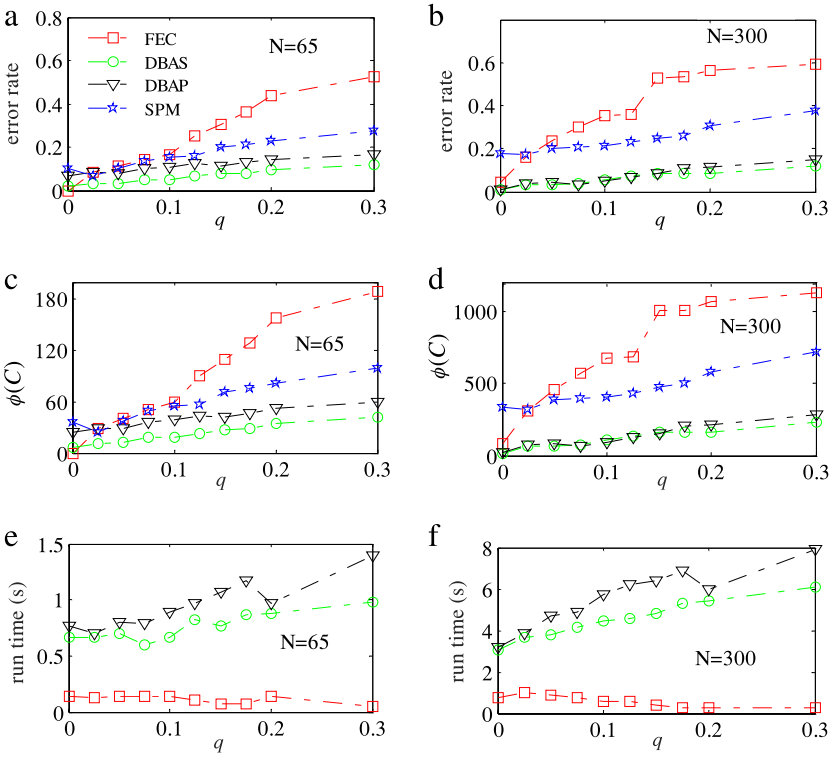

Fig. 17. Comparison of the proposed DBAS with FEC, SPM, and DBAP on networks of $N = 65$ and $N = 300$. For networks of $N = 65$, the parameters are $C_1 = 12$, $C_2 = 15$, $C_3 = 16$, $C_4 = 22$, $N_{th} = 3$, $K_p = 5$, and $K_n = -2.5$. For networks of $N = 300$, the parameters are $C_1 = 60$, $C_2 = 70$, $C_3 = 80$, $C_4 = 90$, $p = 0.6$, $N_{th} = 3$, $K_p = 10$, and $K_n = -1$. (a) Error rate on networks of $N = 65$. (b) Error rate on networks of $N = 300$. (c) ϕ(C) on networks of $N = 65$ ($\alpha = 0.5$). (b) ϕ(C) on networks $N = 300$ ($\alpha = 0.5$). (e) Run time on networks of $N = 65$. (f) Run time on networks of $N = 300$.

Fig. 17(a) and (b) are the error rates of the networks of $N = 65$ and $N = 300$, respectively. The error rate increases as the increasing of q, which indicates that the difficulty to partition is increasing. DBAS always yields lower value of error rate than that of DBSP, indicating that the performance is improved by exploring the information of negative links. Fig. 17(c) and (d) are the ϕ(C) of the networks of $N = 65$ and $N = 300$, respectively. The results coincide with that of Fig. 17(a) and (b). Fig. 17(e) and (f) are the run times of the networks of $N = 65$ and $N = 300$, respectively. The run times of SPM on $N = 65$ and $N = 300$ networks are about 1500 and 10 000 s respectively, which are far more than that of the rest three algorithms, and thus are not shown in Fig. 17(e) and (f). It is seen that the run time of the proposed DBAS increases as the increasing of q.

Simulation 7. Parameters sensitivity experiments.

In this simulation, the 20 networks with $q = 0.1$ and $N = 300$ in Fig. 6(b) of Simulation 6 are used to test the sensitivity of DBAS on the parameters K_p and K_n. To test the sensitivity, we do not reassign the overlapping nodes in the small groups by letting $N_{th} = 0$ (see Step 5 in the method section). Firstly, fixing $K_n = -2$ and varying the value of K_p from 10, 15, 20, 25, and 30, the error rates of the 20 networks are obtained. Fig. 18(a) shows the average value of the 20 networks, which show that the error rate is small when $K_p = 20$. Secondly, fixing $K_p = 20$ and varying the value of K_n from -0.5, -2, -10, -13, and -15, Fig. 18(b) shows the average error rate of the 20 networks. For a given value of K_p (e.g. $K_p = 20$), there is a most appropriate value for K_n ($K_n = -2$ for $K_p = 20$), and vice versa. The observed relation for the appropriate values of K_p and K_n is

$$\frac{K_p}{|K_n|} \approx q. \tag{4}$$

We check relation (4) with $(K_p, K_n) = (10, -1)$, $(20, -2)$, $(30, -3)$, $(40, -4)$, . . . , $(2000, -200)$ on the 20 networks, DBAS works well. The differences are the converging speeds of the phases; $(K_p, K_n) = (10, -1)$ is much faster than that of $(K_p, K_n) = (2000, -200)$.

Relation (4) is helpful for choosing appropriate values of K_p and K_n. But in some real world applications, the value of q may not be available. Relation (4) is not strictly required; in a wide range around q, the two parameters work. In this simulation $N_{th} = 0$. If $N_{th} \neq 0$, the overlapping nodes with $N\_group < N_{th}$ will be reassigned (see Step 5 in the method section), and the sensitivity will be further reduced.

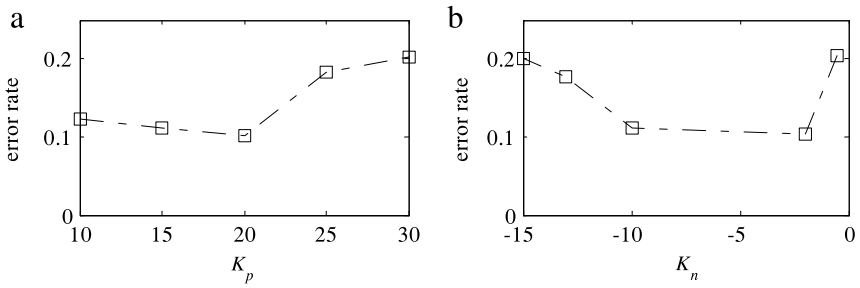

Fig. 18. Parameters sensitivity experiments on networks with $N = 300$, $C_1 = 60$, $C_2 = 70$, $C_3 = 80$, $C_4 = 90$, $p = 0.6$, $N_{th} = 0$, and $q = 0.1$. (a) $K_n = -2$ and K_p varying from 10, 15, 20, 25, and 30. (b) $K_p = 20$ and K_n varying from -0.5, -2, -10, -13, and -15.

6. Conclusion

The WJJLGS model is modified to imitate the evolutionary dynamics of signed social networks. Positive links make the phases of the corresponding individuals evolve together; negative links make the phases of the corresponding individuals evolve far away. As a result, the phases of the signed network evolve into several clusters corresponding to a reasonable partition of the network. Detailed algorithm (DBAS) is also provided. The run time of the algorithm is closely related with the iteration of the differential equation. If the differential equation can be replaced by difference equation, the algorithm could further speed up, which needs further researches.

References

[1] J.J. Jordan, D.G. Rand, S. Arbesman, J.H. Fowler, N.A. Christakis, Contagion of cooperation in static and fluid social networks, PLoS One 8 (6) (2013) e66199.
[2] G. Facchetti, G. Iacono, C. Altafini, Exploring the low-energy landscape of large-scale signed social networks, Phys. Rev. E 86 (2012) 036116.
[3] P. Doreian, A. Mrvar, A partitioning approach to structural balance, Social Networks 18 (1996) 149–168.
[4] B. Yang, W.K. Cheung, J. Liu, Community mining from signed social networks, IEEE Trans. Knowl. Data Eng. 19 (2007) 1333–1348.
[5] M. Girvan, M.E.J. Newman, Community structure in social and biological networks, Proc. Natl. Acad. Sci. USA 99 (2002) 7821–7826.
[6] A. Lancichinetti, F. Radicchi, J.J. Ramasco, S. Fortunato, Finding statistically significant communities in networks, PLoS One 6 (4) (2011) e18961.
[7] Y. Li, H. Wang, J. Li, H. Gao, Efficient community detection with additive constrains on large networks, Knowl.-Based Syst. 52 (2013) 268–278.
[8] M.E.J. Newman, M. Girvan, Finding and evaluating community structure in networks, Phys. Rev. E 69 (2004) 026113.
[9] M.E.J. Newman, Modularity and community structure in networks, Proc. Natl. Acad. Sci. USA 103 (2006) 8577–8582.
[10] Z. Bu, C. Zhang, Z. Xia, J. Wang, A fast parallel modularity optimization algorithm (FPMQA) for community detection in online social network, Knowl.-Based Syst. 50 (2013) 246–259.
[11] S. Cafieri, P. Hansen, L. Liberti, Loops and multiple edges in modularity maximization of networks, Phys. Rev. E 81 (2010) 046102.
[12] G. Xu, S. Tsoka, L.G. Papageorgiou, Finding community structures in complex networks using mixed integer optimization, Eur. Phys. J. B 60 (2007) 231–239.
[13] Y. Qu, W. Shi, X. Shi, Inferring overlapping community structure with degree-corrected block model, Physica A 419 (2015) 48–54.
[14] J. Eustace, X. Wang, Y. Cui, Overlapping community detection using neighborhood ratio matrix, Physica A 421 (2015) 510–521.
[15] J. Shang, L. Liu, X. Li, F. Xie, C. Wu, Epidemic spreading on complex networks with overlapping and non-overlapping community structure, Physica A 419 (2015) 171–182.
[16] I. Leyva, R. Sevilla-Escoboza, J.M. Buldú, I. Sendiña-Nadal, J. Gómez-Gardeñes, A. Arenas, Y. Moreno, S. Gómez, R. Jaimes-Reátegui, S. Boccaletti, Explosive first-order transition to synchrony in networked chaotic oscillators, Phys. Rev. Lett. 108 (2012) 168702.
[17] A. Kocheturov, M. Batsyn, P.M. Pardalos, Dynamics of cluster structures in a financial market network, Physica A 413 (2014) 523–533.
[18] A. Arenas, A. Díaz-Guilera, C.J. Pérez-Vicente, Synchronization reveals topological scales in complex networks, Phys. Rev. Lett. 96 (2006) 114102.
[19] E. Oh, K. Rho, H. Hong, B. Kahng, Modular synchronization in complex networks, Phys. Rev. E 72 (2005) 047101.
[20] T. Zhou, M. Zhao, G.R. Chen, G. Yan, B.H. Wang, Phase synchronization on scale-free networks with community structure, Phys. Lett. A 368 (2007) 431–433.
[21] D. Li, I. Leyva, J.A. Almendral, I. Sendiña-Nadal, J.M. Buldú, S. Havlin, S. Boccaletti, Synchronization interfaces and overlapping communities in complex networks, Phys. Rev. Lett. 101 (2008) 168701.
[22] J.A. Almendral, I. Leyva, D. Li, I. Sendiña-Nadal, S. Havlin, S. Boccaletti, Dynamics of overlapping structures in modular networks, Phys. Rev. E 82 (2010) 016115.
[23] Y. Kao, C. Wang, Global stability analysis for stochastic coupled reaction–diffusion systems on networks, Nonlinear Anal. RWA 14 (2013) 1457–1465.
[24] J. Wu, L. Jiao, C. Jin, F. Liu, M. Gong, R. Shang, W. Chen, Overlapping community detection via network dynamics, Phys. Rev. E 85 (2012) 016115.
[25] J. Wu, R. Lu, L. Jiao, F. Liu, X. Yu, D. Wang, B. Sun, Phase transition model for community detection, Physica A 392 (2013) 1287–1301.
[26] J. Wu, Y. Jiao, Clustering dynamics of complex discrete-time networks and its application in community detection, Chaos 24 (2014) 033104.
[27] Z. Wu, X. Fu, Cluster lag synchronization in community networks via linear pinning control with local intermittent effect, Physica A 395 (2014) 487–498.
[28] L. Chen, Y. Chai, R. Wu, J. Sun, T. Ma, Cluster synchronization in fractional-order complex dynamical networks, Phys. Lett. A 376 (2012) 2381–2388.
[29] C. Hu, H. Jiang, Cluster synchronization for directed community networks via pinning partial schemes, Chaos Solitons Fractals 45 (2012) 1368–1377.
[30] Y. Wang, J. Cao, Cluster synchronization in nonlinearly coupled delayed networks of non-identical dynamic systems, Nonlinear Anal. RWA 14 (2013) 842–851.
[31] N. Bansal, A. Blum, S. Chawla, Correlation clustering, Mach. Learn. 56 (2004) 89–113.
[32] S. Fortunato, Community detection in graphs, Phys. Rep. 486 (2010) 75–174.
[33] T.D. Kaplan, S. Forrest, A dual assortative measure of community structure, 2008. eprint arXiv:0801.3290.
[34] S. Gómez, P. Jensen, A. Arenas, Analysis of community structure in networks of correlated data, Phys. Rev. E 80 (2009) 016114.
[35] V.A. Traag, J. Bruggem, Community detection in networks with positive and negative links, Phys. Rev. E 80 (2009) 036115.
[36] Y. Chen, X.L. Wang, B. Yuan, B.Z. Tang, Overlapping community detection in networks with positive and negative links, J. Stat. Mech. Theory Exp. (2014) P03021.
[37] D. Cartwright, F. Harary, Structural balance: a generalization of Heider's theory, Psychol. Rev. 63 (1956) 277–292.
[38] F. Harary, On the notion of balance of a signed graph, Michigan Math. J. 2 (1953) 143–146.

[39] J.A. Davis, Clustering and structural balance in graphs, Hum. Relat. 20 (1967) 181–187.
[40] P. Doreian, V. Batagelj, A. Ferligoj, Generalized Blockmodeling, Cambridge University Press, New York, 2005.
[41] F. Harary, R.Z. Norman, D. Cartwright, Structural Models, Wiley, New York, 1965.
[42] P. Doreian, A. Mrvar, Partitioning signed social networks, Social Networks 31 (2009) 1–11.
[43] P. Doreian, P. Lloyd, A. Mrvar, Partitioning large signed two-mode networks: Problems and prospects, Social Networks 35 (2013) 178–203.
[44] K.E. Read, Cultures of the central highlands, New Guinea, Southwest. J. Anthropol. 10 (1954) 1–43.
[45] S. Kropivnik, A. Mrvar, An analysis of the Slovene parliamentary parties network, in: Developments in Statistics and Methodology, 1996, pp. 209–216.
[46] L. Wu, X. Ying, X. Wu, A. Lu, Z. Zhou, Examining spectral space of complex network with positive and negative links, Int. J. Soc. Netw. Min. 1 (2012) 91–111.
[47] A.L. Barabási, R. Albert, Emergence of scaling in random networks, Science 286 (1999) 509–512.